PROCEEDINGS OF SCIENCE

Results from the OPERA experiment

Alessandro Paoloni* **on behalf of the OPERA Collaboration**
INFN LNF
E-mail: alessandro.paoloni@lnf.infn.it

The OPERA experiment is an hybrid detector made of nuclear emulsions and of electronic detectors. It has been designed to provide an evidence for $\nu_\mu \to \nu_\tau$ oscillations by detection of τ leptons in the parameter region identified from the observation of atmospheric neutrinos. The experiment took data from 2008 to 2012 on the CNGS beam. In this paper $\nu_\mu \to \nu_\tau$ oscillation results are presented, as well as results from other analyses.

XVI International Workshop on Neutrino Telescopes,
2-6 March 2015
Palazzo Franchetti, Istituto Veneto, Venice, Italy

*Speaker.

© Copyright owned by the author(s) under the terms of the Creative Commons Attribution-NonCommercial-ShareAlike Licence.

PoS(NEUTEL2015)010

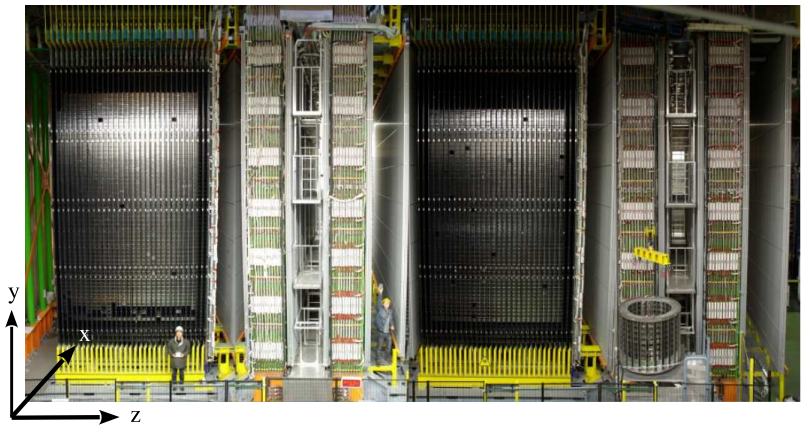

Figure 1: A picture of the OPERA detector.

1. Detector description and data taking.

The OPERA experiment [1] has been designed to detect $\nu_\mu \rightarrow \nu_\tau$ oscillations through τ appearance. A sketch of the detector is shown in figure 1. Its location, inside the underground Gran Sasso laboratories, corresponding to a 732 km long baseline, together with the energy of the CNGS beam, on average 17 GeV, allows covering the Δm^2 region of interest for the atmospheric neutrino oscillations, precisely investigated by SuperKamiokande [2], MINOS [3] and T2K [4].

The detection of the τ leptons, with a decay path $\sim$ mm at the CNGS neutrino energies, is performed by means of the so-called ECC (Emulsion Cloud Chamber) technique, with the neutrino target made by 1 mm thick lead sheets alternated to nuclear emulsions, each one made by two 44 μm layers separated by a plastic base of 200 μm. A stack of 57 emulsion and 56 lead plates constitutes one brick. Bricks are arranged into walls, alternated to modules of *x*-*y* crossed scintillator strips, 2.6 cm wide, read-out by WLS fibers and multi-anode photomultipliers. The scintillator strips, the so-called Target Tracker [5] (TT), are used for the location of bricks with neutrino interactions.

One supermodule is composed by 31 walls and TT layers, followed by a magnetic spectrometer for the rejection of the charm background. The magnetic spectrometer is an iron dipole [6] instrumented with Drift Tubes [7] and Resistive Plate Chambers [8]. The OPERA experiment is made by two supermodules, for a total initial target mass greater than 1.2 kt (corresponding to more than 140000 bricks). The detector was operated on the CNGS neutrino beam from 2008 to 2012, collecting a sample of 19505 contained neutrino interactions out of 17.97×10^{19} pot. Bricks extracted for analysis were not replaced during data taking; the proton-on-target (pot) weighted average mass was 1.18 kt. The decommissioning of the detector has started in January 2015.

2. $\nu_\mu \rightarrow \nu_\tau$ oscillation results.

2.1 τ lepton identification.

Neutrino interactions are selected in coincidence with the CNGS spills ("on-time" events). They are classified as CC-like (Charged Current or "1 μ") and NC-like (Neutral Current or "0 μ")

PoS(NEUTEL2015)010

according to the presence of one reconstructed muon in the electronic detectors. A classifier algorithm, OpCarac [9], is applied to identify the contained events, i.e. those with neutrino interactions inside the OPERA targets.

For each contained event, bricks are ranked according to the probability of containing the neutrino interaction vertex by the brick-finding algorithm [10]. To preserve the detector mass and to save emulsion scanning resources, the bricks had been equipped with an external emulsion Changeable Sheet ("CS") doublet [11] to verify the predictions of the electronic detectors. In absence of confirmation, the following brick in the probability list is analysed. With a positive result from the CS scanning, the emulsions of the brick are developed and the location procedure starts.

Tracks located in the CS are followed back ("scan-back") in the internal emulsions of the brick until a stopping point is found. Scanning an area of about 1 cm^2 in 5 emulsion layers upstream and in 10 emulsion layers downstream of the stopping point ("volume scan") permits the full reconstruction of the neutrino vertex. A decay search procedure ("DS") is then performed aiming at the detection of τ leptons produced in ν_τ^{CC} interactions once a vertex has been identified in the volume scan data [12, 13]. The decay is defined as "short" if it happens either in the same lead plate where the neutrino interaction occurred or in the first downstream emulsion layer and as "long" if it happens further downstream. About 54% of τ decays are expected to be long.

Tracks and showers are finally fully reconstructed inside the brick ("scan forth"). The brick indeed permits to measure the momentum of charged particles sampling the Multiple Coulomb Scattering in the 1 mm thick lead plates [14] and the energy of electro-magnetic showers, as well as to perform particle identification. A kinematic selection is then performed in order to reduce as much as possible the background. Cuts, shown in table 1, are applied on the following quantities:

- z_{dec}: the z-coordinate of the decay vertex with respect to the downstream face of the lead plate containing the primary vertex ($z_{dec} < 44\mu$m for short decays).
- p_T^{miss}: the missing p_T at the neutrino vertex with respect to the beam direction, reconstructed as the vectorial sum of the transverse momenta of the reconstructed particles at the vertex ("primaries").
- ϕ_{lH}: the angle between the τ candidate ("parent") and the vectorial sum of the other primaries calculated in the plane perpendicular to the CNGS axis.
- p^{2ry}: the scalar sum of the momenta of the particles produced in the τ candidate decay ("daughters").
- p_T^{2ry}: the transverse momentum of the daughter with respect to the parent direction, for 1-prong decays.
- p^{2ry}: the scalar sum of the momenta of the daughters.
- θ_{kink}: the average 3D angle between the parent and its daughters (kink angle).
- m: the invariant mass of the daughters (calculated attributing the π mass).
- m_{min}: the minimal invariant mass [15].

PoS(NEUTEL2015)010

variable	$\tau \to 1h$	$\tau \to 3h$	$\tau \to \mu$	$\tau \to e$
lepton-tag		No μ or e at the primary vertex		
z_{dec} (μm)	$[44, 2600]$	< 2600	$[44, 2600]$	< 2600
p_T^{miss} (GeV/c)	$< 1^\star$	$< 1^\star$	/	/
ϕ_{lH} (rad)	$> \pi/2^\star$	$> \pi/2^\star$	/	/
p_T^{2ry} (GeV/c)	$> 0.6(0.3)$*	/	> 0.25	> 0.1
p^{2ry} (GeV/c)	> 2	> 3	> 1 and < 15	> 1 and < 15
θ_{kink} (mrad)	> 20	< 500	> 20	> 20
m, m_{min} (GeV/c^2)	/	> 0.5 and < 2	/	/

Table 1: Kinematic selection. The meaning of the variables is defined in the text. The cut on p_T^{2ry} for the 1-prong hadronic decay is set at 0.3 GeV/c in the presence of γ particles associated to the decay vertex and to 0.6 otherwise. Cuts marked with a $\star$ are not applied in the case of a QE event. Only long decays are considered for the $\tau \to \mu$ and $\tau \to h$ channels due to a large background component in short decays from charmed particles and hadronic re-interactions, respectively.

For events passing the kinematic cuts, tracks are followed in the neighbouring bricks until either a stopping point, an interaction or a muon decay topology is found ("Track follow-down", TFD). Exploiting the momentum-range correlation, the energy loss in proximity of the stopping point and (if possible) the tagging of interactions or muon decays, it is possible to improve the muon/hadron separation with respect to the performances of the electronic detectors. This is crucial to reduce the charm background in all the considered τ decay channels.

2.2 Expectations for signal and background.

A detailed MC simulation has been performed in order to estimate the number of τ and background events.

All particle trajectories are digitised in a volume of $3\times3\times3$ bricks, centered on the brick containing the neutrino interaction. The efficiency and the resolution (in angle and position) of the scanning microscopes are simulated using parametrisations obtained from real data.

The neutrino fluxes estimation is based on a FLUKA simulation of the CNGS beam-line. Neutrino interactions are generated using NEGN tuned with the parameters based on the high-statistics data sample of the NOMAD experiment. The energy-dependence of the ν_τ cross section follows the default GENIE v2.6 implementation. The number of expected oscillations has been computed using a two-neutrino oscillation formula with $\Delta m^2_{32} = 2.32 \times 10^{-3}$ eV^2 [16] and maximal mixing.

The expected number of detectable signal events in the 0μ and 1μ samples are obtained by considering the expected rates of ν_τ^{CC} and ν_μ^{CC} at MC "truth" level and the reconstruction efficiency for standard ν_μ^{CC} achieved for real data. Migrations of NC and CC events within the 0μ and 1μ samples are taken into account (see [18] for more details). The predictions thus obtained are insensitive to systematic effects on the efficiencies being common to ν_τ and ν_μ events. A similar approach is also used in the estimation of backgrounds.

Three sources of background are expected to give a significant contribution to the number of selected candidates:

- **Charmed particles decay.** Charmed particles production is mostly associated with ν_μ^{CC} interactions. This background is strongly suppressed tagging the muon produced in the neu-

PoS(NEUTEL2015)010

	Observed candidates	Signal events $\Delta m^2_{32} = 2.32\text{m}(\text{eV}^2)$	All backgrounds	Charm background	LAS background	Hadronic background
$\tau \to h$	2	0.41 ± 0.08	0.033 ± 0.006	0.015 ± 0.003	/	0.018 ± 0.005
$\tau \to 3h$	1	0.57 ± 0.11	0.155 ± 0.030	0.152 ± 0.030	/	0.002 ± 0.001
$\tau \to \mu$	1	0.52 ± 0.10	0.018 ± 0.007	0.003 ± 0.001	0.014 ± 0.007	/
$\tau \to e$	0	0.62 ± 0.12	0.027 ± 0.005	0.027 ± 0.005	/	/
all	4	2.11 ± 0.42	0.233 ± 0.041	0.198 ± 0.040	0.014 ± 0.007	0.021 ± 0.006

Table 2: Signal and background expectations for the analysed sample.

year	2008	2009	2010	2011	2012	total
pot	1.74	3.53	4.09	4.75	3.86	17.97
0μ events	148	250	209	223	149	979
1μ events ($p_\mu < 15$ GeV/c)	534	1019	814	749	590	3706
all events	682	1269	1023	972	739	4685

Table 3: Summary of the analysed data samples.

trino interaction vertex. It contributes to all the τ decay channels considered for the analysis, but for decays into muons, it can be further suppressed by requiring a negative muon charge.

- **Hadronic re-interactions.** Hadronic interactions in 0μ events can mimick the topology of a single or three-prong τ decay. The kinematic selection strongly reduces this contamination due to the typical low transverse momentum of the secondary products and the reduced flight length of hadrons (the typical hadronic interaction length is much larger than the τ decay length). A further reduction is obtained by requiring the absence of nuclear fragments in the decay vertex.

- **Large angle Coulomb scattering.** The occurrence of large-angle scattering of muons in thin ($\mathcal{O}(0.1)X_0$) lead plates is, at present, not well constrained by measurements; experimental and simulation activities to determine this process are in progress. Here the same contribution used for the experiment proposal ($1 \times 10^{-5}/\nu_\mu^{CC}$) is assumed.

The expected number of signal and background events are summarized in table 2.

Consistency checks have been performed by comparing data and MC distributions. As an example, in figure 2 the location efficiency is shown as a function of the energy reconstructed in the TT [18]. Charmed particles, given the similarities in mass and decay topologies with the τ lepton, have also been used as a control sample [13].

2.3 Observed events and statistical significance.

The sample of events analyzed so far consists of the highest probability bricks, for all 0μ events and for 1μ events with a muon momentum $p_\mu < 15$ GeV/c. In addition, for 2008-2009 CNGS runs also the second probability bricks have been analysed for all events (even those with $p_\mu > 15$ GeV/c which are anyway not considered in the τ analysis.) A summary is given in table 3; the analyzed data correspond roughly to about 70% of the total sample.

The collaboratoin has so far reported the observation of four events, shown in figure 3. The first [17] is a candidate for $\tau \to \rho\nu_\tau$ (single prong hadronic decay). The second [18] is a three

PoS(NEUTEL2015)010

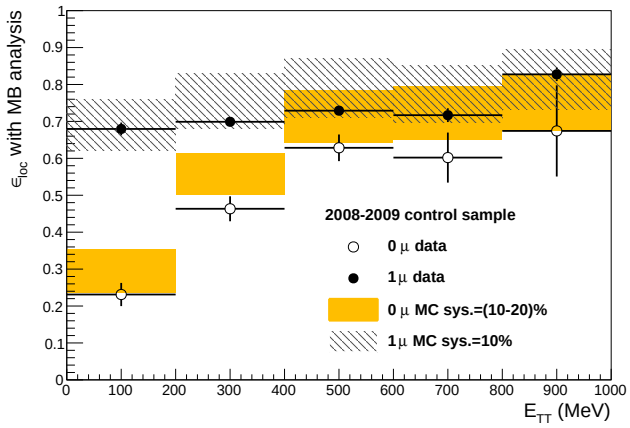

Figure 2: Location efficiency with the two-brick analysis (ε_{loc}) vs E_{TT} in a control sample of data collected in 2008 and 2009 (bullets) compared with MC (histograms). The comparison is done separately for 0μ and 1μ events. The error bars represent the systematical and statistical uncertainties in the MC and in the data respectively.

prong decay candidate. The third [19] is a muonic decay candidate, the only oscillation event so far in which the charge of the final lepton has been reconstructed with high precision. The fourth candidate [20] is another single prong hadronic decay.

The significance of the observation of the four ν_τ candidate events is estimated by considering the confidence for excluding the null hypothesis. Two calculations based on a Fisher combination and a likelihood-ratio approach [20] yield very close results at 4.2 σ. No shape information is used but just a simple counting of the observed and expected background events in each channel.

3. Results from other analyses.

3.1 Limits on $\nu_\mu \to \nu_\tau$ oscillations induced by a sterile neutrino.

The observation of four events is compatible with the expectation of 2.33 ± 0.42 events and therefore limits can be derived on the existence of a fourth sterile neutrino [21]. The $\nu_\mu \to \nu_\tau$ oscillation probability is modified by the existence of the additional sterile neutrino, i.e.:

$$\begin{aligned} P(\nu_\mu \to \nu_\tau) &= 4|U_{\mu 3}^2||U_{\tau 3}^2| \sin^2 \frac{\Delta_{31}}{2} + 4|U_{\mu 4}^2||U_{\tau 4}^2| \sin^2 \frac{\Delta_{41}}{2} \\ &+ 2\mathscr{R}[U_{\mu 4}^* U_{\tau 4} U_{\mu 3} U_{\tau 3}^*] \sin\Delta_{31} \sin\Delta_{41} - 4\mathscr{I}[U_{\mu 4}^* U_{\tau 4} U_{\mu 3} U_{\tau 3}^*] \sin^2 \frac{\Delta_{31}}{2} \sin\Delta_{41} \\ &+ 8\mathscr{R}[U_{\mu 4}^* U_{\tau 4} U_{\mu 3} U_{\tau 3}^*] \sin^2 \frac{\Delta_{31}}{2} \sin^2 \frac{\Delta_{41}}{2} + 4\mathscr{I}[U_{\mu 4}^* U_{\tau 4} U_{\mu 3} U_{\tau 3}^*] \sin\Delta_{31} \sin^2 \frac{\Delta_{41}}{2} \end{aligned} \quad (3.1)$$

where U_{ij} is an extended 4×4 PMNS matrix and $\Delta_{ij} = 1.27\Delta m_{ij}^2 \frac{L}{E}$. Depending on the values assumed by the extra terms in the U matrix an enhancement or a suppression of the expected ν_τ can occur.

For $|\Delta m_{41}^2| > 1\text{eV}^2$, a limit of 0.116 has been obtained on $\sin^2 2\theta_{\mu\tau} = 4|U_{\mu 4}|^2|U_{\tau 4}|^2$ at 90% CL. Figure 4, left, shows the log likelihood ratio as a function of $\sin^2 2\theta_{\mu\tau}$ for $\phi_{\mu\tau} = Arg(U_{\mu 3} U_{\tau 3}^* U_{\mu 4}^* U_{\tau 4}) =$

PoS(NEUTEL2015)010

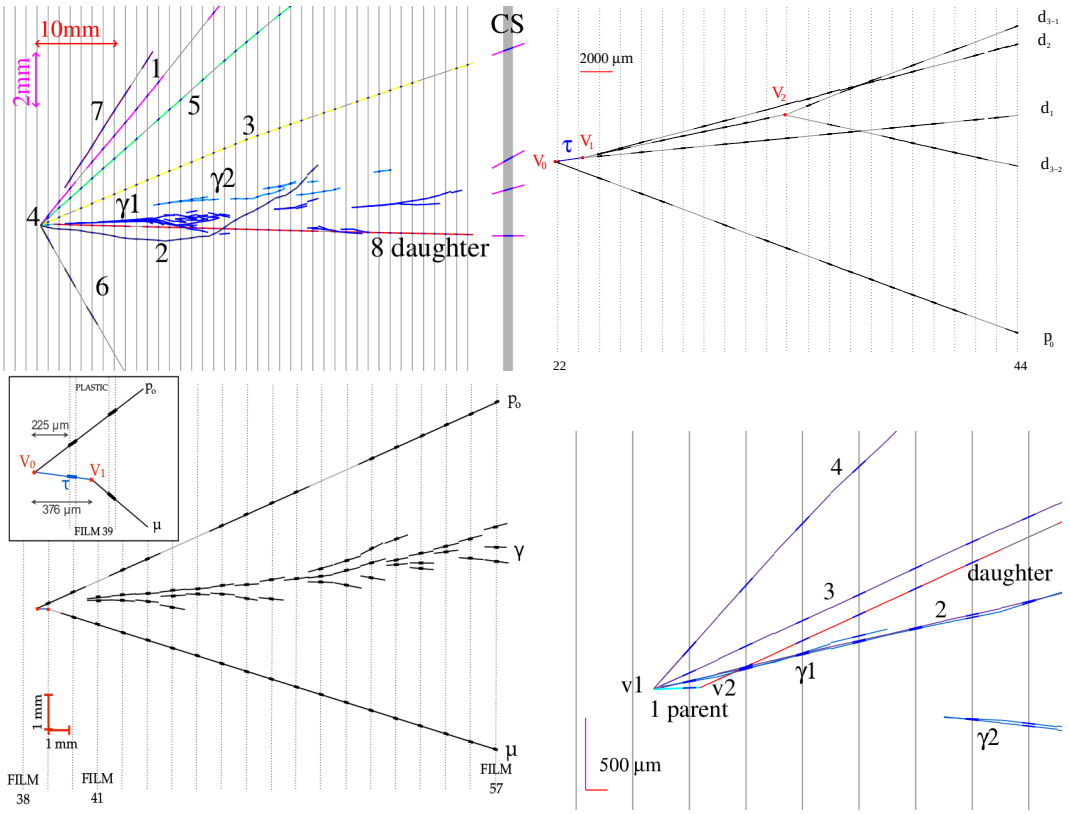

Figure 3: Side view inside the brick of the four (so far) observed ν_τ candidates. Vertical lines indicate the position of emulsion films, numbered in increasing order, from 1 to 57. The pitch is 1.3 mm. Top left: $\tau \to 1h$ candidate [17]. Top right: $\tau \to 3h$ candidate [18]. Bottom left: $\tau \to \mu$ candidate [19]. Bottom right: $\tau \to 1h$ candidate [20].

0 (dashed line) and after profiling the likelihood on $\phi_{\mu\tau}$ (continuous line). The right plot in the same figure shows the 90% C.L. exclusion region in the $|U_{\tau 4}|^2$ vs $|U_{\mu 4}|^2$ plane.

Using the GLoBES software [22, 23], which takes into account the non-zero Δm^2_{21} value and also matter effects, limits on $\sin^2 2\theta_{\mu\tau}$ have been extended also down to small positive Δm^2_{41} values, and are shown in figure 5. Small differences are observed for the two hierarchies of the three standard neutrinos. For negative Δm^2_{41} values, the exclusion plots are similar but with hierarchies exchanged. In the plot, the results of CHORUS [24] and NOMAD [25], are also shown for comparison.

3.2 $\nu_\mu \to \nu_e$ oscillation results.

Exploiting the excellent electron reconstruction capabilities of the ECCs, the OPERA experiment is suited also for the detection of $\nu_\mu \to \nu_e$ oscillations. Using the data from the 2008/2009 runs 19 ν_e candidates were observed with an expected background of 19.8 ± 2.8 [26]. In figure 6, left, the distribution of the reconstructed energy of the 19 ν_e candidates is shown, compared with the expected reconstructed energy spectra from the ν_e beam contamination, the oscillated ν_e from the three-flavour oscillations and the background (NC interactions with associated π^0s and $\tau \to e$ events), normalised to the analysed pot. Below 20 GeV, 4.2 events from ν_e beam contamination

PoS(NEUTEL2015)010

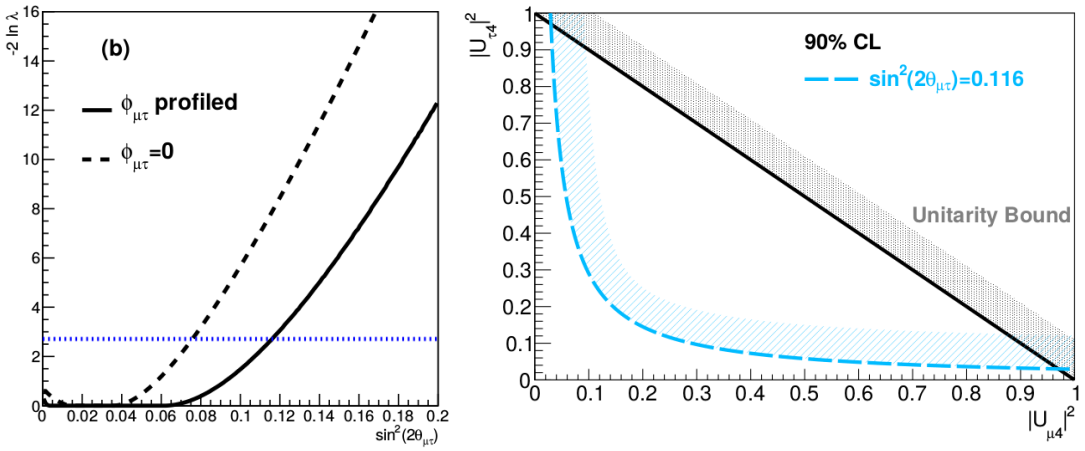

Figure 4: Left: Log likelihood ratio vs $\sin^2 2\theta_{\mu\tau}$ for $\phi_{\mu\tau} = 0$ (dashed line) and for the profile likelihood (continuous line). Right: 90% CL exclusion limits (blue line) in the $|U_{\tau 4}|^2$ vs $|U_{\mu 4}|^2$ plane assuming $\Delta m^2_{41} > 1\text{eV}^2$. The unitarity bound (black line) is also shown. Bands are drawn to indicate the excluded regions.

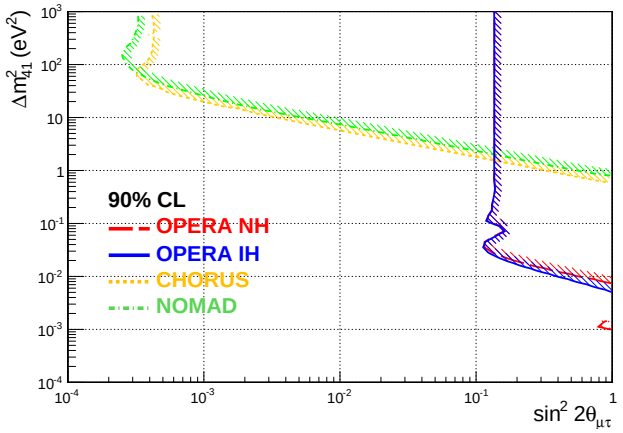

Figure 5: OPERA 90% CL exclusion limits in the Δm^2_{41} vs $\sin^2 2\theta_{\mu\tau}$ parameter space for the normal (NH, dashed red) and inverted (IH, solid blue) hierarchy of the three standard neutrino masses. The exclusion plots by NOMAD [25] and CHORUS [24] are also shown. Bands are drawn to indicate the excluded regions.

and 0.4 events from other backgrounds are expected. The expected signal from the θ_{13} driven oscillations is 1.0 event and 4 candidates are observed yielding $\sin^2(2\theta_{13}) < 0.44$ at 90% CL. The possible contribution from a sterile neutrino state has been assessed by parametrising the transition probability with a 2-flavour formula with an effective mixing angle. The observation translates into a 90% C.L. upper limit on $\sin^2 2\theta_{\text{eff}}$ at 7.2×10^{-3} (Fig. 6, right).

3.3 Measurement of the muon charge ratio.

The underground Gran Sasso laboratory is a privileged location to study TeV-scale muons from cosmic rays interactions in the atmosphere. A sample of more than 3 milion muon events have been reconstructed (including charge measurement) by the OPERA electronic detectors, among which 110000 multiple muon bundles. The charge ratio $R_\mu = N_{\mu^+}/N_{\mu^-}$ has been measured separately for

PoS(NEUTEL2015)010

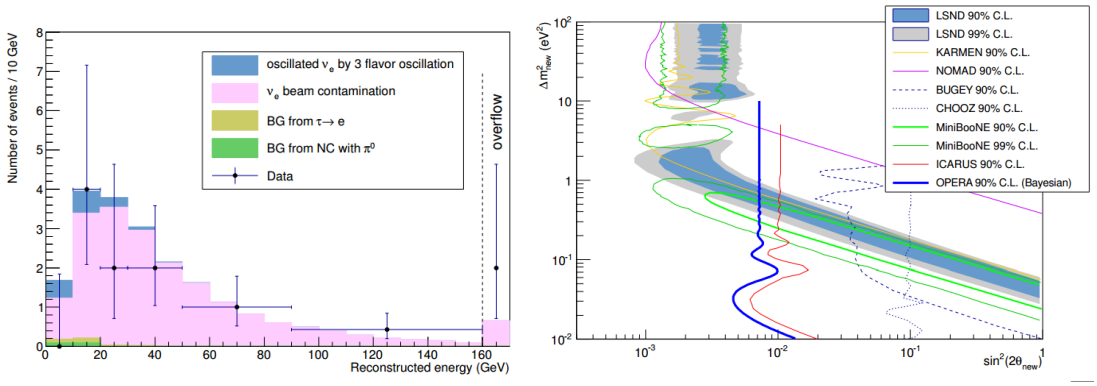

Figure 6: Left: Distribution of the reconstructed energy of the observed ν_e events; the stacked histogram shows the expected spectrum from different sources, normalised to the number of analysed pot. Right: The exclusion plot for the parameters of the non-standard $\nu_\mu \rightarrow \nu_e$ oscillation, obtained from this analysis using the Bayesian method, is shown.

single and for multiple muon events [27]:

$$R_\mu(n_\mu = 1) = 1.377 \pm 0.006(\text{stat.})^{+0.007}_{-0.001}(\text{syst.}) \tag{3.2}$$

$$R_\mu(n_\mu > 1) = 1.098 \pm 0.023(\text{stat.})^{+0.015}_{-0.013}(\text{syst.}) \tag{3.3}$$

In figure 7 the charge ratio for single muon events is shown as a function of the surface energy up to 20 TeV. R_μ is well described by a parametric model including only pion and kaon contribution to the muon flux, showing no significant contribution of the prompt component (i.e. muons from charm decays).

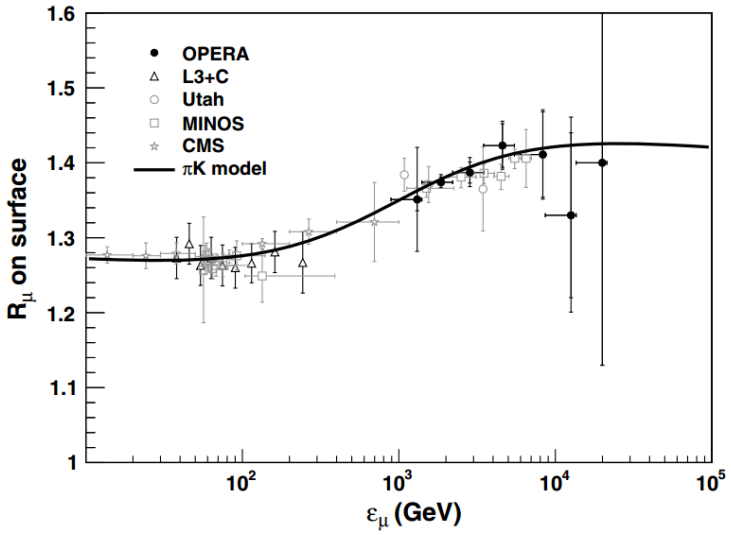

Figure 7: Measurement of the muon charge ratio as a function of the surface energy E_μ (black points). The result of a fit including only pion and kaon contribution to the muon flux is also shown as a continuous line.

PoS(NEUTEL2015)010

References

[1] R. Acquafredda *et al.*, JINST **4**, P04018 (2009).

[2] R. Wendell *et al.* (Super-Kamiokande Collaboration), Phys. Rev. D 81, 092004 (2010).

[3] P. Adamson *et al.* (MINOS collaboration), Phys. Rev. Lett. 110, 251801 (2013).

[4] K. Abe *et al.* (T2K Collaboration), Phys. Rev. Lett. 112, 181801 (2014).

[5] T. Adam *et al.*, Nucl. Instrum. Meth. A 577, 523 (2007).

[6] M. Ambrosio *et al.*, IEEE TNS Vol.51 n.3, 975 (2004).

[7] R. Zimmermann *et al.*, Nucl. Instrum. Meth. A 555, 435 (2005).

[8] A. Paoloni *et al.*, PoS(RPC2012), 010 (2012).

[9] A. Bertolin *et al.*, OPERA public note n. 100 (2009).

[10] A. Chukanov *et al.*, OPERA public note n. 162 (2013).

[11] A. Anokhina *et al.*, JINST **3**, P07005 (2008).

[12] A. Ariga *et al.*, OPERA public note n.128 (2011).

[13] N. Agafonova *et al.*, Eur. Phys. J. C74, 2986 (2014).

[14] N. Agafonova *et al.*, New J. Phys. 14, 013026 (2012).

[15] E.L. Berger *et al.*, Phys. Lett. B 140, 259 (1984).

[16] K. Nakamura *et al.*, J. Phys. G 37, 075021 (2010).

[17] N. Agafonova *et al.*, Phys. Lett. B 691, 138 (2010).

[18] N. Agafonova *et al.*, New J. Phys. 14 033017 (2012).

[19] N. Agafonova *et al.*, Phys. Rev. D 89, 051102 (2014).

[20] N. Agafonova *et al.*, PTEP 10, 101C01 (2014).

[21] N. Agafonova *et al.*, arXiv:1503.01876 submitted to JHEP.

[22] P. Huber, M. Lindner and W. Winter, Comput. Phys. Commun. 167, 195 (2005).

[23] P. Huber, J. Kopp, M. Lindner, M. Rolinec and W. Winter, Comput. Phys. Commun. 177, 432 (2007).

[24] E. Eskut *et al.*, Nucl. Phys. B 793, 326 (2008).

[25] P. Astier *et al.*, Nucl. Phys. B 611 3 (2001).

[26] N. Agafonova *et al.*, JHEP 07, 004 (2013).

[27] N. Agafonova *et al.*, Eur. Phys. J. C 74, 2933 (2014).

PoS(NEUTEL2015)010